Fluorescence spectroscopic measurements in methane/air and hydrogen/oxygen atmospheric pressure flames in the excitation wavelength range of 303 nm to 240 nm

by

R. Stocker, J. Karl, D. Hein

Lehrstuhl für Thermische Kraftanlagen

Technische Universität München

D-85747 Garching, Boltzmannstr. 15, Germany

ABSTRACT

Laser induced fluorescence (LIF) is a well-known technology to detect different species in combustion processes. One of the most important species is the OH radical, which provides information about combustion kinetics, flame front etc. An other component, the pollutant NO, responsible for the formation of unhealthy ozone O_3 is formed in different kinds of flames.

In the presented work the flame of a methane/air Bunsen burner and a flame of a hydrogen/oxygen welding torch, are investigated, using a laser diode pumped Nd:YAG laser system, tuneable in the UV wavelength range of 325 nm to 210 nm. The tuning device of the laser consists of an OPO (Optical Parametric Oscillator, Type II) and a frequency-doubling device (SHG, Second Harmonic Generator). The laser output frequency has a bandwidth of ≈15 cm^{-1}. What we aim at with this paper is to show the application possibilities of a tunable OPO laser system in flame research.

In order to find appropriate electronic transitions to excite combustion species like OH, NO or O_2 for selective laser-induced fluorescence measurements, the excitation wavelength range from 303 nm to 240 nm (excitation frequency: 33003 cm^{-1} to 41667 cm^{-1}) was scanned. The transitions of the hydroxyl radical $A^2\Sigma^+ \leftarrow X^2\Pi$ (1,0), (2,0) and (3,0) bands could be excited and were investigated more intensely. Detected OH LIF (laser-induced fluorescence) signals of the (1,0) band are about one hundred times more intense than LIPF (laser-induced predissociative fluorescence) signals of the (3,0) band. With the high fluorescence signal intensity of the OH (1,0) band, it is possible to get images of 2-dimensional time-resolved qualitative OH distribution. In Fig. 1 a 2-dimensional time-resolved OH LIF measurement of a methane/air Bunsen burner flame is shown. The excitation frequency of the Nd:YAG laser was set to 38322 cm^{-1}.

In addition, laser-induced fluorescence of nitrogen monoxide in the $A^2\Sigma^+ \leftarrow X^2\Pi$ (0,2) transition was detected. It is shown, that it is possible to excite NO selectively with the tunable Nd:YAG laser described in the paper.

The results of these investigations are aimed to support an application of the laser system in a combustion chamber, where industrial burners of up to 200 kW thermal output could be analyzed.

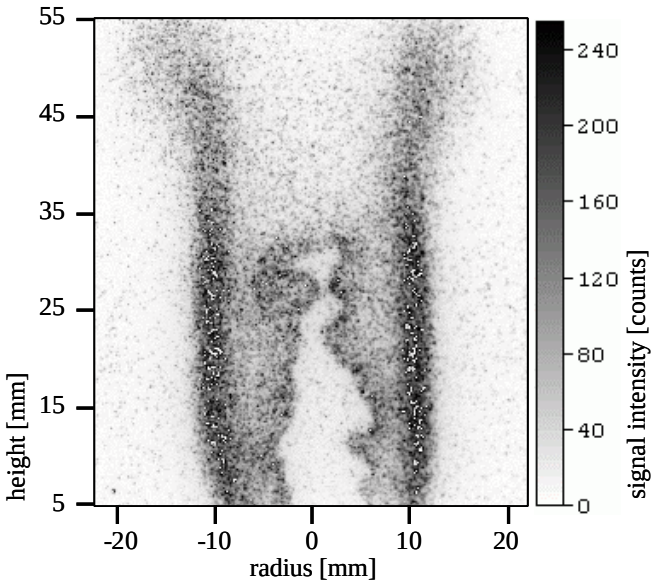

Fig. 1: OH LIF single shot measurement in a methane/air Bunsen burner flame. Excitation frequency at 38322 cm^{-1}.

1. INTRODUCTION

One of the most important species in combustion processes is the OH radical, which provides information about combustion kinetics, flame front etc. Nitrogen oxide formed in combustion processes contributes to environmental pollution. Laser induced fluorescence (LIF) is a well-known technology to detect different species, like OH, NO and O_2 [1],[2],[3].

In the excitation wavelength range from 303 nm down to 240 nm several transitions of OH ($A^2\Sigma^+$) and NO ($A^2\Sigma^+$) are found.

[4] and [5] describe the excitation of OH ($A^2\Sigma^+$), v' = 1 in atmospheric pressure flames. LIF measurements of turbulent premixed flames in a high-pressure environment are shown in [6]. Laser-induced fluorescence detection of the OH ($A^2\Sigma^+$), v' = 2 transition in atmospheric pressure flames are described in [7], [8]. The visualization and detection of hydroxyl radicals in different flames with excitation of OH ($A^2\Sigma^+$), v' = 3 transition were applied in [9], [10], [11], [12].

[13], [14] and [15] show laser-induced fluorescence of the pollutant nitrogen monoxide. Transitions of NO $A^2\Sigma^+$ (0,2) in acetylene/oxygen flames, in engines and in flames of furnances are excited.

Measurements in a large scale facility is presented in [16] by laser-induced fluorescence imaging in a 100 kW natural gas flame.

In the present work a flame of a methane/air Bunsen burner and a flame of a hydrogen/oxygen welding torch, are investigated. The pulsed laser system consists of a laser diode pumped Nd:YAG laser with Second Harmonic Gerneration (SHG) and Third Harmonic Generation (THG), a tunable OPO (Optical Parametric Oscillator, Type II) and a frequency-doubling device (SHG, Second Harmonic Generation). The laser system is tuneable in the UV wavelength range from 325 nm to 210 nm. The aim of this paper is to show the possibilities of application of the tunable OPO laser system in flame research.

In order to find appropriate electronic transitions to excite combustion species like OH, NO or O_2 for selective laser-induced fluorescence measurements, the excitation wavelength range from 303 nm to 240 nm (excitation frequency: 33003 cm^{-1} to 41667 cm^{-1}) was scanned. Fig. 2 shows an excitation-emission spectrum (EES) of a methane/air Bunsen burner flame. The laser excitation wavelength was tuned from 303 nm down to 240 nm, the emission wavelength of Rayleigh scattering and laser-induced fluorescence is displayed between 200 nm and 410 nm.

In the upper part of Fig. 2 transitions of OH ($A^2\Sigma^+$) (1,0) band can be seen (excitation wavelength: ≈ 291 nm to 278.5 nm). The signals in the middle section of the EES are transitions from OH ($A^2\Sigma^+$) (2,0) band (excitation wavelength: ≈ 271 nm to 259 nm) and in the lower part OH ($A^2\Sigma^+$) (3,0) transitions are shown (excitation wavelength: ≈ 251 nm to 242 nm). NO ($A^2\Sigma^+$) transitions cannot be seen in the figure. These three excitation ranges are investigated further in this paper.

The results of these investigations are aimed at supporting an application of the laser system in a combustion chamber, where industrial burners with a thermal output up to 200 kW can be analyzed.

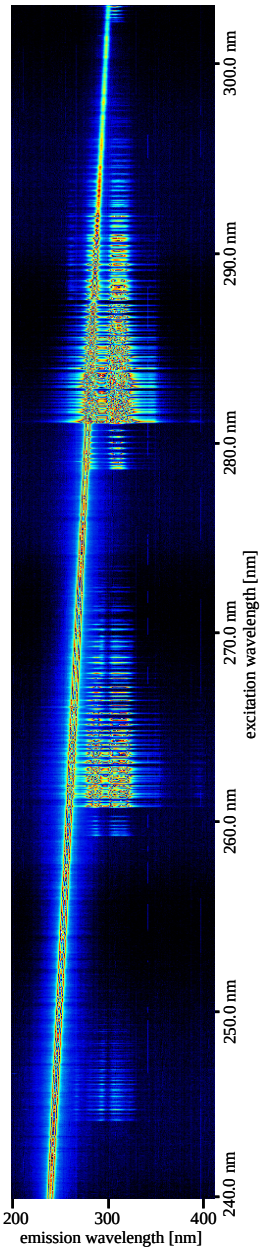

Fig. 2: Excitation-emission spectrum of a methane/air flame. The laser excitation wavelength is tuned from 303 nm down to 240 nm.

2. EXPERIMENTAL SETUP and PROCEDURES

2.1 Flames considered

The experiments described in this paper are focused on methane/air and hydrogen/oxygen flames. The methane/air flame is combusted using a commercial Bunsen burner, flame diameter ≈30 mm and height ≈110 mm. The hydrogen/oxygen is burnt with a commercial welding torch, flame diameter ≈7 mm and height ≈200 mm. The hydrogen/oxygen flame of a welding torch offers the advantage of much higher temperature and correspondingly larger OH number density. Combustion took place at ambient pressure and air/oxygen ratios above 1.

2.2 Experimental Setup

Fig. 3 shows a scheme of the experimental setup. A pulsed laser system is used (Infinity-XPO laser, Coherent). The laser diode pumped Nd:YAG laser generates a pulse with the fundamental wavelength of 1064 nm. The repetition rate is variable in the range of 0 to 100 Hz. The pulse is amplified by two Nd:YAG rods, the pulse energy accounts up to 500 mJ. After the passage of the pulse throught the amplifying system, it is sent through

the SHG (Second Harmonic Generation), an angle tuned BBO crystal (Beta Barium Borate). In the crystal, the infrared radiation undergoes doubling. The polarization of the fundamental remains unchanged while the polarization of the second harmonic at 532 nm is perpendicular to the incoming fundamental. After a waveplate (not shown in Fig. 3), the two beams of 1064 nm and 532 nm are sent through a second angle tuned BBO crystal (THG, Third Harmonic Generation) where they undergo a frequency mixing. The radiation produced at 354,7 nm is thereafter separated from the infrared and doubled radiation. The pulse energy rates up to 160 mJ.
In a tunable Optical Parametric Oscillator (OPO, Type II), light at 354,7 nm is injected in a crystal, which provides light of two other wavelengths, the "signal" and the "idler". In the experiments, only the signal wavelength is used. The signal wavelength is tuneable from 709.4 nm to 420 nm, dependent on the angle position of the crystal. After the OPO, the SHG arrangement allows doubling of the OPO signal wavelength. Therefore, in the UV-range the pulsed laser system is tuneable from 325 nm down to 210 nm. At the wavelength of 240 nm to 300 nm the maximum UV laser energy of a single shot is about 5 mJ. The pulse duration is 3 ns in average and the laser bandwidth of a single shot measures 15 cm^{-1}.

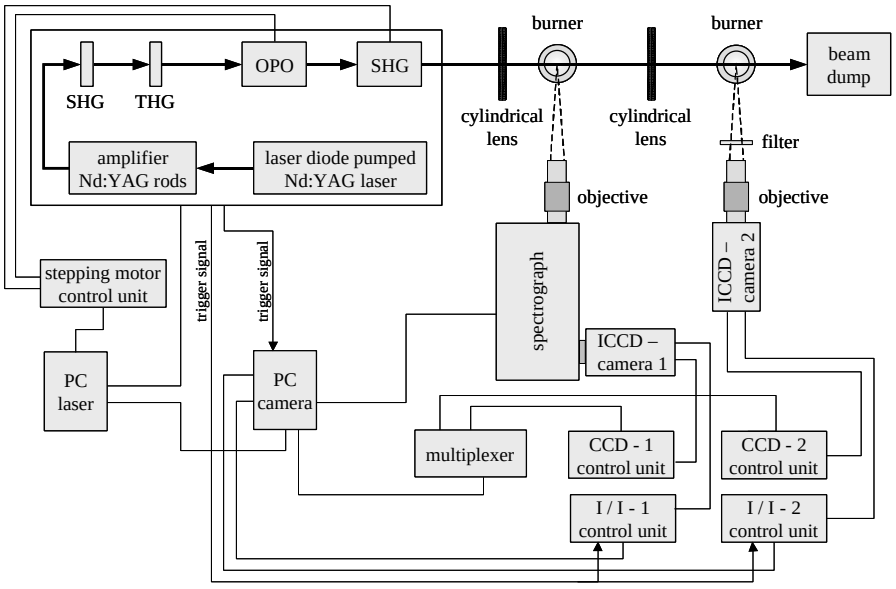

Fig. 3: Experimental setup for spectrally resolved or time-resolved laser-induced fluorescence (LIF) measurements in different flames.

The laser beam is focused by a cylindrical convex lens. Behind the first burner (methane/air Bunsen burner or hydrogen/oxygen welding torch) a second cylindrical convex lens transforms the UV laser beam to a laser sheet of 60 mm height and 0,5 mm width. This laser sheet crosses the second burner, a methane/air Bunsen burner or hydrogen/oxygen burner (in some experiments also symmetric-convex lenses are used).
In the experiments, two intensified CCD cameras (ICCD) were used (FlameStar, LaVision). The camera includes an UV-sensitive gateable microchannel plate image intensifier (I/I) and a slow scan CCD sensor with 16-bit dynamic range. ICCD camera 1 delivers information about wavelength and position of excited molecules using an UV-light permeable objective, focal length 105 mm and f/4,5 aperture (UV Nikkor, Nikon) and an imaging spectrograph (250IS, CHROMEX). The spectrograph is a 250-mm-focal-length, f/4.0 aperture ratio model equipped with three different gratings. In this work the gratings with 1200 grooves/mm, blaze wavelength 200 nm and 100 grooves/mm, blaze wavelength 450 nm were used. The spectrograph is mounted with the entrance slit (50 µm) oriented parallel to the laser beam's propagation direction . The spectral system response was calibrated using a mercury argon lamp.
The second ICCD camera permits spatial-resolved and time-resolved 2D-images of different flames. Rayleigh scattering light was separated from LIF signal with UV transmitting black glass filters (UG11 and UG5, Melles Griot).
The two CCD control units and two I/I control units are controlled by a personal computer (PC camera). With a second computer (PC laser), the laser system is managed and the crystals in the OPO and SHG are rotated via a stepping motor control unit in order to vary laser output wavelength. The laser system provides a trigger signal for the camera system and the image intensifier (I/I units).

2.3 Experimental Procedure

To record the excitation-emission spectra (EES), the laser beam is focused two centimetres outside the flame front/reaction zone in order to avoid two-photon photo dissociation of H_2O [13]. The measurements in the methane/air flame are carried out in the reaction zone, 20 mm above the Bunsen burner. In the hydrogen/oxygen flame, investigation took place in the reaction zone 50 mm above the welding torch.
For each line of the EES, shown in the chapters 3.1, 3.2 and 3.3, 60 laser pulses were summed up and signal intensities of the reaction zone were averaged. The laser wavelength was tuned in 0.01 nm steps.
The laser bandwidth was checked with an excitation scan at the rotational line $P_1(8)$ of the hydroxyl radical $A^2\Sigma^+$ (v' = 3) ← $X^2\Pi$ (v" = 0) transition and amounts to circa 15 cm^{-1} at 248 nm.

3. MEASUREMENTS, RESULTS and DISCUSSION

Three excitation wavelength ranges are studied deeper: First the range from 251.0 nm to 242.0 nm, secondly the range from 291.0 nm to 278.5 nm and finally the range from 271.0 nm to 259.0 nm.

3.1 Investigations in the Range of 251.0 nm to 242.0 nm

In the range of 251.0 nm down to 242.0 nm initial investigations with methane/air flames showed that the fluorescence signals of diverse molecules and radicals are weak because of the low pulse energy of about 5 mJ of the laser. In order to get higher temperatures and correspondingly a higher OH number density. Further experiments were done with a hydrogen/oxygen flame of a welding torch.

Fig. 4 displays the excitation-emission spectrum (EES) of the hydrogen/oxygen flame. The excitation frequency of the laser was tuned from 39.841 cm^{-1} until 41.322 cm^{-1} and the detected emission wavelength in the EES reaches form 224 nm to 298 nm. The tuning range of the KrF excimer laser, 248.9 nm to 247.7 nm (40.175 cm^{-1} to 40.375 cm^{-1}) is situated within the scanned area.

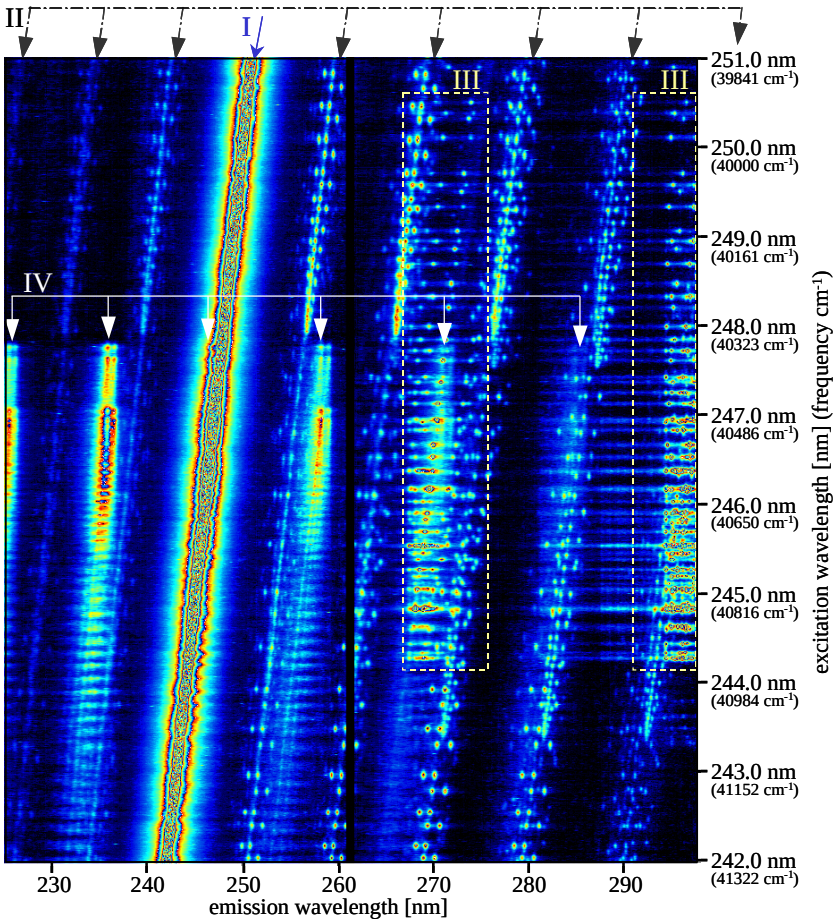

Fig. 4: Excitation-emission spectrum of a hydrogen/oxygen flame. Excitation wavelength is tuned from 251.0 nm until 242.0 nm. The emission wavelength is detected from 224 nm to 300 nm.

In the excitation-emission spectrum of Fig. 4 different signals: Rayleigh scattering, LIF and LIPF are detected. The line of the elastic Rayleigh scattering signal (labeled I) starts at an emission wavelength of 251 nm at the upper side of the figure and ends at an emission wavelength of 242 nm at the bottom respectively to the excitation frequency of the laser. Rayleigh scattering interferes with fluorescence signals of diverse molecules and radicals.

At the upper edge of Fig. 4 (excitation frequency of about 39.850 cm^{-1}) vibrational bands at ≈226 nm, ≈233 nm, ≈241 nm, ≈259 nm, ≈268 nm, ≈279 nm and ≈289 nm are detected in the spectral range of 224 nm to 300 nm. These emissions, labeled with II, parallel to the Rayleigh line are transitions from Schumann-Runge bands of molecular oxygen O_2. They correspond to the transition from the ground state $^3\Sigma_g^-$ to the higher electronic state $^3\Sigma_u^-$ ($B^3\Sigma_u^- \leftarrow X^3\Sigma_g^-$). The electronic B state $^3\Sigma_u^-$ is predissociative. Intensive electronic transitions are within the (0,6), (1,6), (2,7), (3,7), (4,8), (5,8), (6,9) and (7,9) bands. In the excitation range of 39840 cm^{-1} to 40330 cm^{-1} there are several rotational lines, where it is possible to detect only hot oxygen in a hydrogen/oxygen flame [17].

In area III of Fig. 4 (rectangular broken lines) laser-induced predissociative fluorescence LIPF of hydroxyl $A^2\Sigma^+$ (v' = 3) ← $X\ ^2\Pi$ (v'' = 0) transitions are detected [13], [18]. In the left rectangle OH LIPF ($A^2\Sigma^+$ - $X\ ^2\Pi$) of (3,1) and (2,0) band transitions are shown. The lower vibrational levels are populated by vibrational energy transfer (VET) after excitation. In the upper left corner and lower right corner, OH fluorescence superposes LIPF of hot oxygen (Schumann-Runge bands). The right rectangle of area III shows hydroxyl laser-induced predissociative fluorescence ($A^2\Sigma^+$ - $X^2\Pi$) of (1,0), (2,1) and (3,2) bands. In addition, this OH fluorescence signals interfere with oxygen LIPF.

Furthermore, OH LIPF interferes with fluorescence of nitrogen monoxide starting at an excitation frequency of about 40330 cm^{-1}, labeled IV. In the outside region of the exhaust stream ambient air mixes into the hot gas flow and thus nitrogen oxide is formed. Nitrogen monoxide LIF is described further below.

Fig. 5 shows an excitation spectrum of OH $A^2\Sigma^+$ (v' = 3) ← X $^2\Pi$ (v'' = 0) in a hydrogen/oxygen flame within the excitation frequency range from 39841 cm^{-1} to 41322 cm^{-1}. Fluorescence signals are averaged in the emission wavelength interval from 294.0 nm to 297.5 nm. Because of the laser bandwidth of about 15 cm^{-1} it is mostly not possible to excite single rotational lines of the OH $A^2\Sigma^+$ ← X $^2\Pi$ transition. As a consequence the peaks in Fig. 5 displays simultaneous excitation of several rotational lines of OH.
The transitions within the tuning range of the EES are identified with the program LIFBASE (SRI International) [19]. The peaks in Fig. 5 are labeled with the names of the most intensive rotational lines within the respective

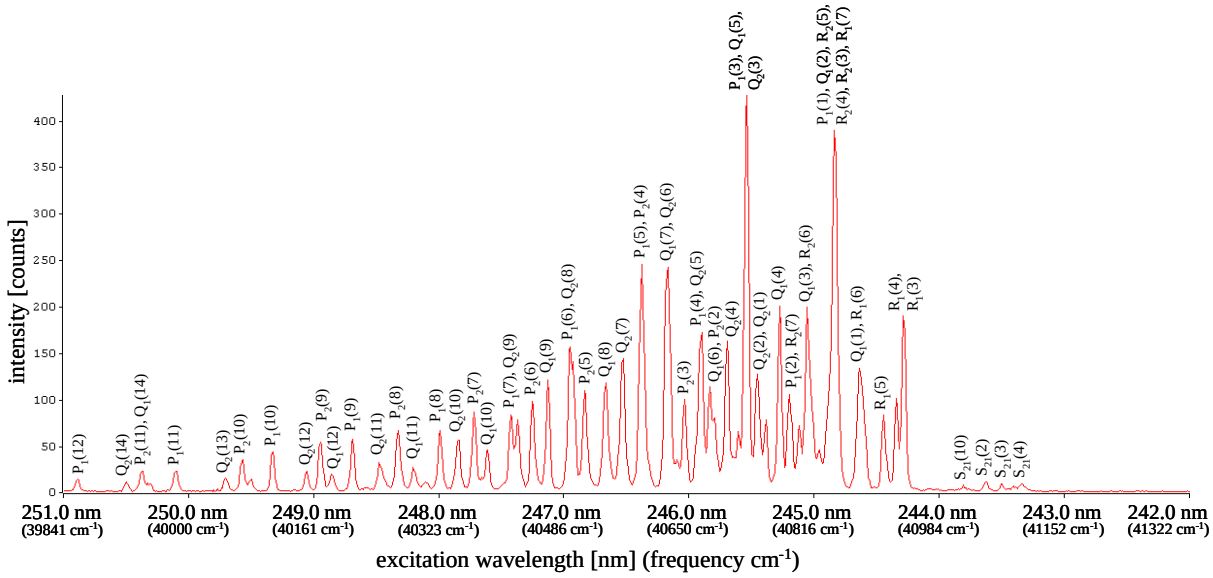

Fig. 5: Excitation spectrum of OH A^2S^+ (v' = 3) ¬ X ^{2}P (v'' = 0) transitions in a hydrogen/oxygen flame within the excitation frequency range from 39841 cm^{-1} to 41322 cm^{-1}. Fluorescence signals are averaged in the emission wavelength interval from 294.0 nm to 297.5 nm.

peak. For example, at the peak labeled $P_1(5)$, $P_2(4)$ the rotational lines of $P_1(5)$, $P_2(4)$, $R_2(11)$, $O_{12}(3)$ and $P_{12}(4)$ are simultaneously excited. The rotational lines $R_2(11)$, $O_{12}(3)$ and $P_{12}(4)$ however hardly influence peak intensity.
Using the excitation lines $P_1(9)$ and $R_1(3)$, the calibration of the laser excitation frequency was checked, as these lines have no superposition with other rotational lines. For $P_1(9)$ the calculated excitation frequency amounts to 40193.47 cm^{-1} the measurement results in 40211 cm^{-1}. At the rotational line $R_1(3)$ the deviation of measurement from calculation amounts to 30 cm^{-1}.
Due to the interference of OH $A^2\Sigma^+$ (v' = 3) ← $X^2\Pi$ (v'' = 0) transitions with O_2 LIPF or NO LIF within the excitation range, it is not possible to excite OH radicals selective with the OPO laser system. Only in cases with no NO formation it is possible to detect OH selectively. In this case, useable rotational lines are $Q_1(8)$, $P_1(5)$ with $P_2(4)$ and $Q_1(7)$ with $Q_2(6)$.
As already mentioned, ambient air mixes into the hydrogen/oxygen flame and thus nitrogen oxide is formed. In the range investigated, several NO transitions can be excited. The transitions of $B^2\Pi$ (v' = 1) ← $X^2\Pi$ (v'' = 3), $B^2\Pi$ (v' = 3) ← $X^2\Pi$ (v'' = 4) and $B^2\Pi$ (v' = 2) ← $X^2\Pi$ (v'' = 4), which have rotational lines in the detected range can not be observed in the experiment. This is due to the thermal population distribution. The vibrational levels (v'' = 3) and (v'' = 4) in the electronic ground state are poorly populated. They are not enough populated to detect excitation of NO molecules to the electronic B state.
Furthermore there are several rotational lines of the $A^2\Sigma^+$ (v' = 0) ← $X^2\Pi$ (v'' = 2) transition of nitrogen monoxide [13] which can be detected because of the sufficient thermal population of the vibration level (v'' = 2). Fig. 4 shows NO $A^2\Sigma^+$ (v' = 0) ← $X^2\Pi$ (v'' = 2) laser-induced fluorescence, labeled IV, starting at a laser excitation frequency of about 40330 cm^{-1} .
In a first step peaks of NO fluorescence in the excitation-emission spectrum of Fig. 4 were identified with the computer program LIFBASE. After that it was attempted to find useful peaks, where it is possible to excite nitrogen monoxide selectively. Fig. 6 displays an excitation spectrum of nitrogen monoxide $A^2\Sigma^+$ ← X $^2\Pi$ (0,2) and (1,3) transitions in a hydrogen/oxygen flame within the excitation frequency range from 39841 cm^{-1} to 41322 cm^{-1}. For the profile the LIF signals were averaged in the emission wavelength interval from 234.5 nm to 237.5 nm in the (0,1) band. This paper does not present results, whether the rotational lines of $A^2\Sigma^+$ (v' = 1) ← $X^2\Pi$ (v'' = 3) transition, starting at an excitation frequency of 40850 cm^{-1}, are involved in the peaks detected.
The identification of the NO peaks showed that at each detected peak several rotational lines were excited simultaneously. In this work the peaks labeled (1), (2), (3) and (4) as well as the regions (5) and (6) shown in Fig. 6 are identified. These peaks and regions are selected, because of their high fluorescence signal intensity and be-

cause of the negligible interferences with fluorescence signals of other molecules or radicals at the excitation frequencies of (3), (4), (5) and (6).

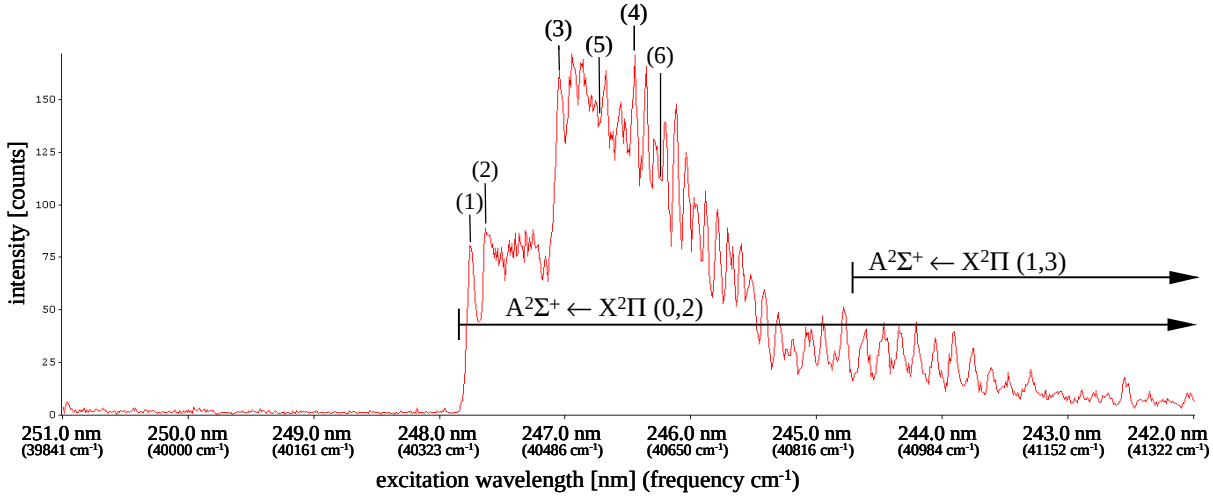

Fig. 6: Excitation spectrum of nitrogen monoxide $A^2S^+ \neg X^2P$ (0,2) and (1,3) transitions in a hydrogen/oxygen flame within the excitation frequency range from 39841 cm^{-1} to 41322 cm^{-1}. LIF signals are averaged in the emission wavelength interval from 234.5 nm to 237.5 nm in the (0,1) band.

Rotational lines [19]:

Peak (1): $P_{12}(9.5)$, $P_{12}(8.5)$, $P_{12}(10.5)$, $P_{12}(7.5)$, $P_{12}(11.5)$, $P_{12}(6.5)$, $P_{12}(12.5)$, $P_{12}(5.5)$, $P_{12}(13.5)$, $P_{12}(4.5)$, $P_{12}(14.5)$, $P_{12}(3.5)$, $P_{12}(15.5)$, $P_{12}(2.5)$, $P_{12}(16.5)$, $P_{12}(1.5)$

Peak (2): $P_12(17.5)$, $P_2(2.5)$, $Q_{12}(2.5)$, $P_2(3.5)$, $Q_{12}(3.5)$, $P_2(1.5)$, $Q_{12}(1.5)$, $P_2(4.5)$, $Q_{12}(4.5)$, $P_2(5.5)$, $Q_{12}(5.5)$, $P_{12}(18.5)$, $P_2(6.5)$, $Q_{12}(6.5)$, $P_2(7.5)$, $Q_{12}(7.5)$, $Q_2(1.5)$, $R_{12}(1.5)$, $P_{12}(19.5)$, $P_2(8.5)$, $Q_{12}(8.5)$, $Q_2(2.5)$, $R_{12}(2.5)$, $P_2(9.5)$, $Q_{12}(9.5)$

Peak (3): $R_2(9.5)$, $P_1(8.5)$, $P_1(7.5)$, $R_{12}(14.5)$, $Q_2(14.5)$, $P_1(9.5)$, $P_1(6.5)$, $P_1(10.5)$, $P_1(5.5)$, $P_{12}(29.5)$, $P_1(11.5)$, $P_1(4.5)$, $Q_{12}(21.5)$, $P_2(21.5)$, $P_1(12.5)$, $P_1(3.5)$, $R_2(10.5)$,$P_1(13.5)$, $P_1(2.5)$, $R_{12}(15.5)$, $Q_2(15.5)$, $P_1(14.5)$

Peak (4): $R_{12}(24.5)$, $Q_2(24.5)$, $P_{12}(38.5)$, $R_1(15.5)$, $Q_{21}(15.5)$, $P_1(28.5)$, $Q_1(21.5)$, $P_{21}(21.5)$, $R_2(19.5)$, $R_{21}(11.5)$, $Q_{12}(31.5)$, $P_2(31.5)$

Region (5): $R_1(9.5)$, $Q_{21}(9.5)$, $R_{12}(20.5)$, $Q_2(20.5)$, $Q_1(15.5)$, $P_{21}(15.5)$, $R_2(15.5)$, $P_1(23.5)$, $R_{21}(6.5)$, $R_1(10.5)$, $Q_{21}(10.5)$, $Q_{12}(27.5)$, $P_2(27.5)$, $Q_1(16.5)$, $P_{21}(16.5)$, $P_{12}(35.5)$, $R_{12}(21.5)$, $Q_2(21.5)$, $P_1(24.5)$

Region (6): $P_2(32.5)$, $Q_1(23.5)$, $P_{21}(23.5)$, $P_1(30.5)$, $R_{21}(13.5)$, $R_{12}(26.5)$, $Q_2(26.5)$, $P_{12}(40.5)$, $R_2(21.5)$, $R_1(18.5)$, $Q_{21}(18.5)$, $Q_1(24.5)$, $P_{21}(24.5)$, $Q_{12}(33.5)$, $P_2(33.5)$, $P_1(31.5)$

In the excitation frequency ranges of peak (1) (40332 cm^{-1} to 40350 cm^{-1}) and peak (2) (40350 cm^{-1} to 40368 cm^{-1}) seen in Fig. 6, nitrogen monoxide, hot oxygen molecules and hydroxyl radicals are excited simultaneously (see also Fig. 4). Therefore in these areas there are no suitable conditions for two-dimensional imaging of NO.
As already mentioned above, in the excitation frequency ranges of (3) (40451 cm^{-1} to 40470 cm^{-1}), (4) (40592 cm^{-1} to 40607 cm^{-1}), (5) (40531 cm^{-1} to 40548 cm-^{1}) and (6) (40628 cm^{-1} to 40644 cm^{-1}) there is no or slight interference with fluorescence of other species as seen in Fig. 7. The figure shows an emission spectrum of a hydrogen/oxygen flame at an excitation frequency of about 40.460 cm^{-1} (peak 3). Bands of nitrogen monoxide transitions $A^2\Sigma^+ - X^2\Pi$ and Rayleigh signal are marked. Maximum measured intensities of NO fluorescence are at wavelength of: ≈225.5 nm (0,0) band, ≈235.9 nm (0,1) band, ≈247.1 nm (0,2) band and Rayleigh scattering, ≈258.2 nm (0,3) band, ≈270.9 nm (0,4) band and ≈284,9 nm (0,5) band. Especially at the ranges of peak (3) and (4) it should be possible to get two-dimensional images of nitrogen monoxide.

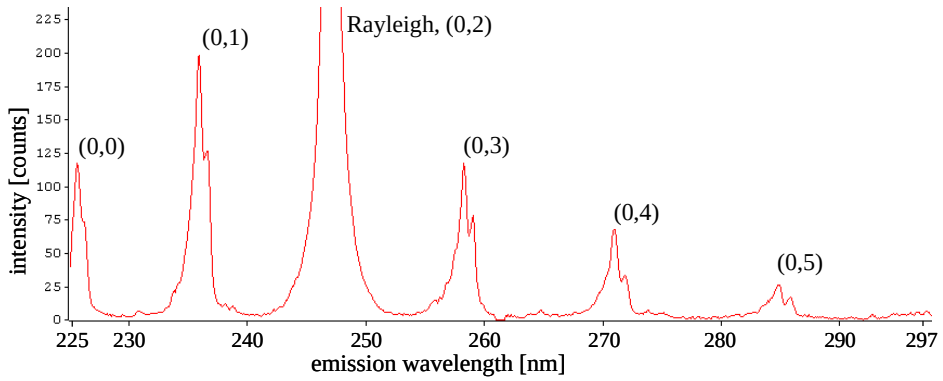

Fig. 7: Emission spectrum of a hydrogen/oxygen flame at an excitation frequency of 40460 cm^{-1}. Emissions of nitrogen monoxide in the A^2S^+ - X^2P transition and Rayleigh signal are shown.

3.2 Investigations in the Range of 291.0 nm to 278.5 nm

The flame of a methane/air Bunsen burner was investigated in the excitation wavelength range of 291.0 nm to 278.5 nm (34364 cm^{-1} to 35907 cm^{-1}). The laser beam was focused with a symmetric-convex lens (Suprasil 1, Heraeus), focal length 150 mm. The focus of the laser beam was about two centimetres outside the region investigated. Fluorescence and Rayleigh signals are averaged in the flame front/reaction zone of the Bunsen burner

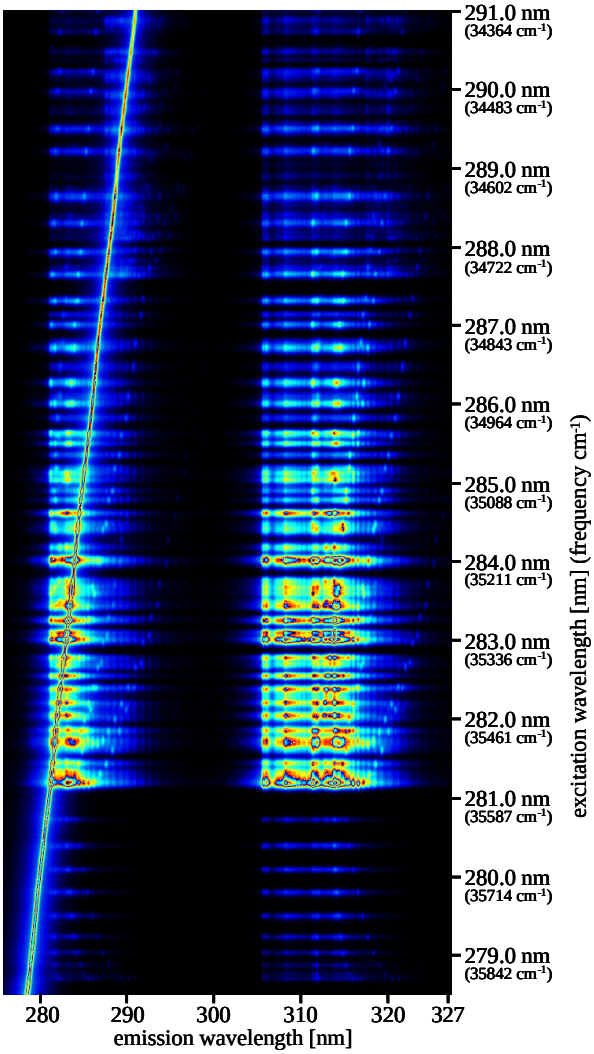

Fig. 8: Excitation-emission spectrum of a methane/air Bunsen burner flame. The excitation wavelength is tuned from 291.0 nm to 278.5 nm, the emissions are detected from 275 nm to 327 nm.

In Fig. 8 an excitation-emission spectrum of a methane/air flame is shown. The excitation wavelength is tuned from 291.0 nm down to 278.5 nm. The emission wavelength is detected from 275 nm to 327 nm. The EES is recorded with the 1200 grooves/mm grating. Outside the emission wavelength range displayed in Fig. 8 no further fluorescence signals could be observed.

The signals in the excitation-emission spectrum could be identified as laser-induced fluorescence of hydroxyl radicals. In the tuned excitation range electronic transitions of hydroxyl are $A^2\Sigma^+$ (v' = 1) ← $X^2\Pi$ (v'' = 0) and $A^2\Sigma^+$ (v' = 2) ← $X^2\Pi$ (v'' = 1) [18]. The excitation of OH in the (1,0) band starts at a calculated excitation frequency of 35877 cm^{-1}, rotational lines are found in the whole range. Transitions in the (2,1) band start at a calculated excitation frequency of 35044 cm^{-1}. In comparison to the rotational lines of the (1,0) band, transitions in the (2,1) band have a low intensity.

In the left part of Fig. 8 there is superposition of Rayleigh scattering (slope) and OH fluorescence ($1 \rightarrow 0$) band. Beginning with an emission wavelength of about 305 nm OH fluorescence in the ($0 \rightarrow 0$) and ($1 \rightarrow 1$) bands are found in the right section of the EES.

In search of the most intensive transitions of the hydroxyl radical in order to visualize OH distribution in different flames the rotational lines of the $A^2\Sigma^+ \leftarrow X^2\Pi$ (1,0) and (2,1) transitions were identified with the computer program LIFBASE [19].

Fig. 9 displays an excitation spectrum of OH in a methane/air flame within the excitation wavelength range from 291.0 nm to 278.5 nm. Fluorescence signals are averaged in the emission wavelength interval from 305 nm to 317 nm, ($0 \rightarrow 0$) and ($1 \rightarrow 1$) bands. Because of the bandwidth of the laser ($\approx$ 15 cm^{-1} at 287 nm), the discrete OH peaks result from excitation of several rotational lines at the same time. OH peaks are lettered with the rotational lines concerned. The most intensive electronic transitions of each peak are colored red, bold and italic. Transitions with less intensity are labeled in normal letters. Rotational lines, which does not appear or appear with low intensity are typed in italic only. The lines within each peak are indexed by excitation frequency (higher excitation frequency first). In Fig. 9 a few rotational lines within the (2,1) band are highlighted in grey.

The excitation spectrum presented in Fig. 9 shows that, because of their high signal intensity, peaks labeled 1, 2, 3, 4 and 5 are especially suited to detect OH and image an qualitative OH distribution. Most important rotational lines of the peaks are:

	Main rotational lines	Measured maximum value at [cm^{-1}]	Calculated value [cm^{-1}]
Peak 1	$R_1(5)$, $R_1(6)$, $R_1(4)$, $R_1(7)$, $R_1(3)$, $R_1(8)$	35562	$R_1(7)$ 35553.99
Peak 2	$R_1(10)$, $R_2(7)$, $R_2(6)$, $R_2(8)$, $R_2(5)$	35499	$R_2(6)$ 35500.59
Peak 3	$Q_1(6)$, $Q_2(3)$	35333	$Q_1(6)$ 35334.38
Peak 4	$Q_2(5)$, $Q_1(7)$	35303	$Q_1(7)$ 35297.62
Peak 5	$Q_1(9)$, $Q_2(8)$, $P_1(5)$	35208	$Q_2(8)$ 35210.20

To record 2-dimensional spatial-resolved OH distribution it is necessary to separate OH LIF from Rayleigh scattering with adequate filters. Because of superposition of Rayleigh signals and fluorescence in the ($1 \rightarrow 0$) band, the signals of the (1,0) band can not be used for spatial OH detection. However the high intensity of the emission in the ($0 \rightarrow 0$) and ($1 \rightarrow 1$) bands allows to measure distribution of hydroxyl radicals in flames.

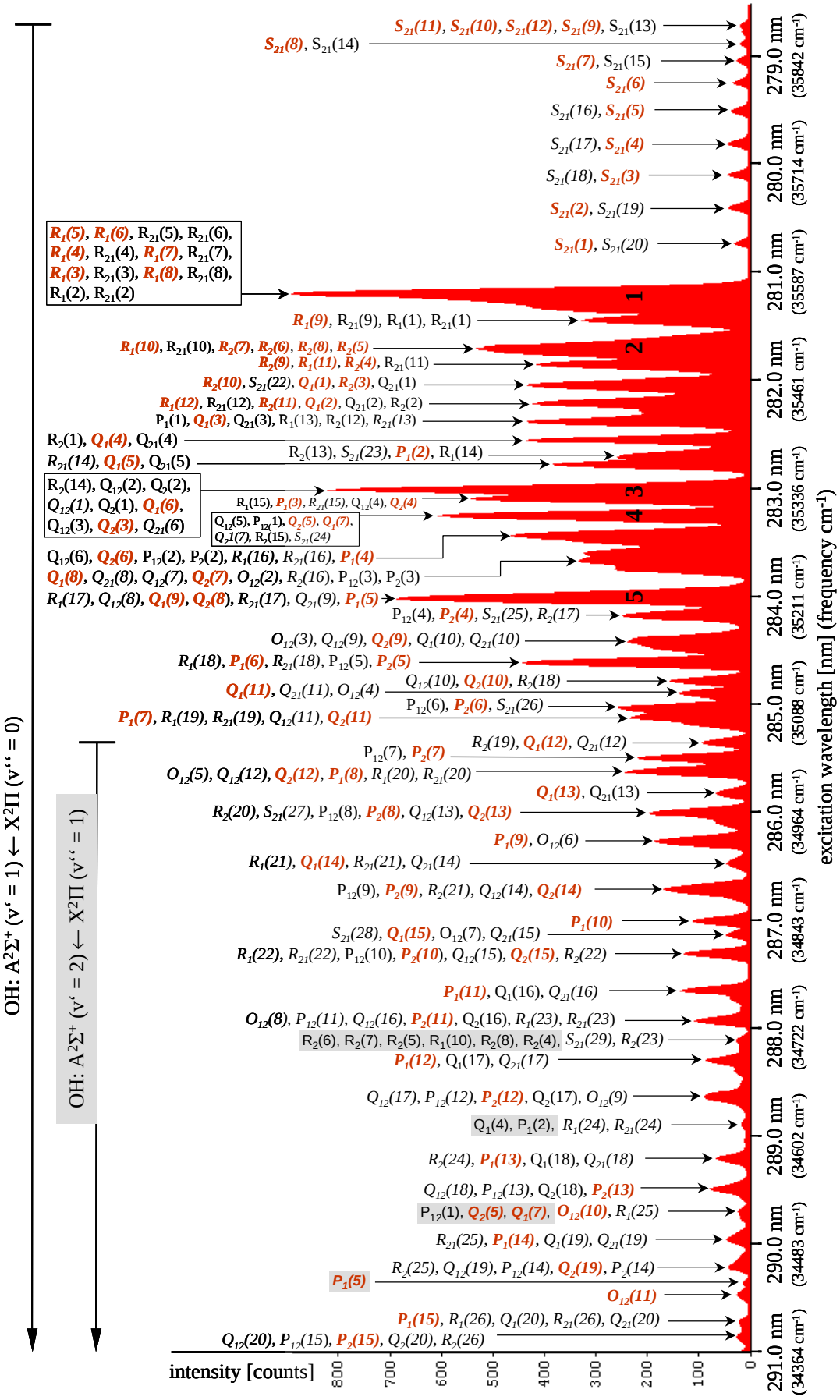

Fig. 9: Excitation spectrum of hydroxyl in a methane/air flame within the excitation wavelength range from 291.0 nm to 278.5 nm. Fluorescence signals are averaged in the emission wavelength interval from 305 nm to 317 nm. OH peaks are labeled with the rotational lines concerned.

3.3 Investigations in the Range of 271.0 nm to 259.0 nm

Furthermore in the excitation wavelength range of 271.0 nm to 259.0 nm (36900 cm^{-1} to 38610 cm^{-1}) the methane/air flame of a Bunsen burner was investigated. The experimental setup was the same as described in the tuning range of chapter 3.2. The gain of the image intensifier was increased because of lower intensity of the fluorescence signal. With a symmetric-convex lens (focal length of 150 mm) the laser beam is focused about two centimetres outside the flame front / reaction zone of the Bunsen burner.

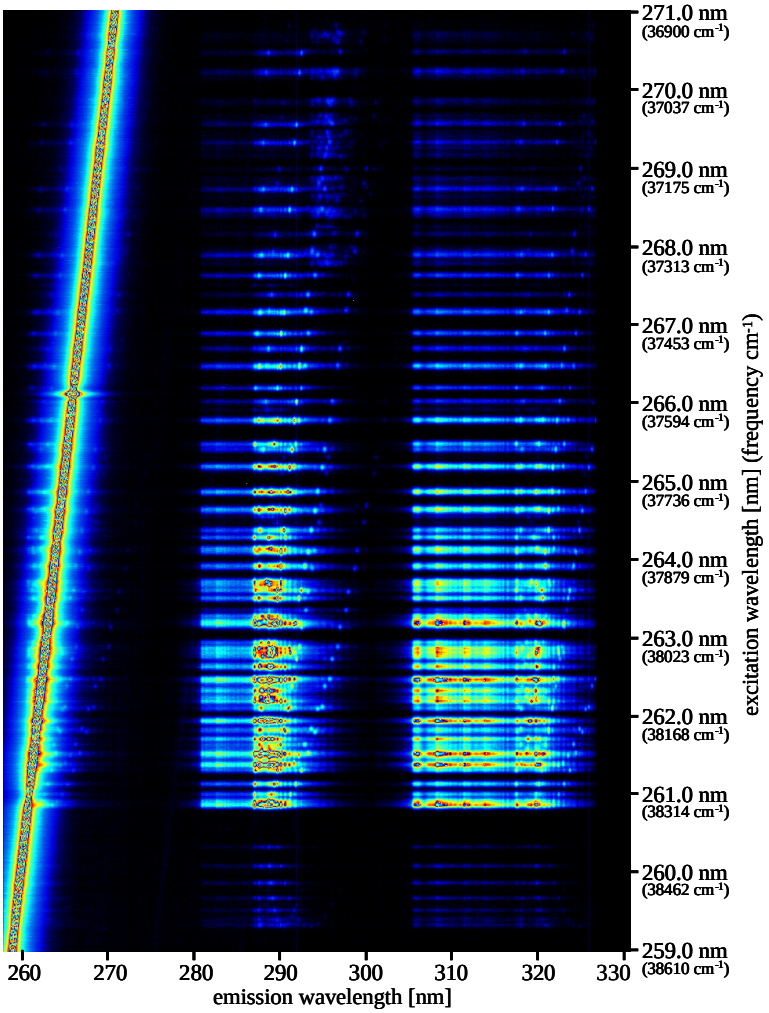

Fig. 10: Excitation-emission spectrum of a methane/air flame. Excitation wavelength is tuned from 271.0 nm to 259.0 nm. The emission wavelength is detected from 258 nm to 330 nm.

An excitation-emission spectrum of a methane/air flame is displayed in Fig. 10. The excitation wavelength of the laser is tuned form 271.0 nm to 259.0 nm. In the experiment a 1200 grooves/mm grating is used. The emission wavelength is displayed from 258 nm to 330 nm. At wavelength higher then 330 nm no further emissions were detected.

Two transition bands of OH are located within the tuned range of the laser wavelength. First there is the OH $A^2\Sigma^+$ (v' = 2) ← $X^2\Pi$ (v'' = 0) transition (LIF) [18]. Rotational lines start at a calculated excitation frequency of 38553 cm^{-1}, transitions of the (2,0) band are found in the whole tuning range of Fig. 10 [19]. Second hydroxyl radicals of the flame can be excited in the $A^2\Sigma^+$ (v' = 3) ← $X^2\Pi$ (v'' = 1) transition (LIPF). The excitation in the (3,1) band is predissociative and in comparison to the (2,0) band signals of low intensity [19]. In the left part of Fig. 10 Rayleigh scattering (slope) and superposition of Rayleigh scattering and OH fluorescence in the $(2 \rightarrow 0)$ band is seen. The middle section shows LIF of $(1 \rightarrow 0)$ and $(2 \rightarrow 1)$ bands. Detected emissions between 305 nm and 330 nm are from $(0 \rightarrow 0)$, $(1 \rightarrow 1)$ and $(2 \rightarrow 2)$ transitions ((3,1) LIPF not considered).

Fig. 11 shows an excitation spectrum of OH in a methane/air flame within the excitation wavelength range of 271.0 nm to 259.0 nm. LIF and LIPF signals are averaged in the emission wavelength interval from 286.5 nm to 290.7 nm. The location of rotational lines within the (2,0) and (3,1) band are represented. OH peaks are lettered with the rotational lines concerned. The most intensive electronic transitions within each peak are colored red, bold and italic. Transitions with less intensity are labeled in normal print. Rotational lines, which do not appear or appear with low intensity are typed in italic only. The lines within each peak are indexed by excitation frequency (higher excitation frequency first). In Fig. 11 rotational lines within the OH (3,1) band are highlighted in grey.

Transitions with highest intensity are labeled 1, 2, 3, 4, 5 and 6. The most important rotational lines within each peak are:

	Main rotational lines	Measured maximum value at [cm^{-1}]	Calculated value [cm^{-1}]
Peak 1	$R_1(3)$, $R_1(4)$, $R_1(2)$, $R_{21}(2)$, $R_1(5)$, $R_1(1)$	38333	$R_1(2)$ 38321.98
Peak 2	$R_1(8)$, $Q_1(1)$, $Q_{21}(1)$, $R_2(5)$, $R_2(4)$, $R_2(6)$	38258	$R_2(5)$ 38251.75
Peak 3	$R_2(3)$, $R_2(7)$, $Q_1(2)$, $Q_{21}(2)$, $R_1(9)$	38238	$Q_1(2)$ 38230.18
Peak 4	$Q_1(4)$, $P_1(2)$	38177	$P_1(2)$ 38169.20
Peak 5	$Q_2(4)$, $Q_1(6)$	38101	$Q_1(6)$ 38092.05
Peak 6	$Q_2(7)$, $Q_1(8)$, $P_1(5)$	37995	$Q_1(8)$ 37988.78

Within the $A^2\Sigma^+$ (v' = 2) ← $X^2\Pi$ (v'' = 0) excitation for qualitative measurements of OH distribution in methane/air or hydrogen/oxygen flames the peaks mentioned above are suited best.

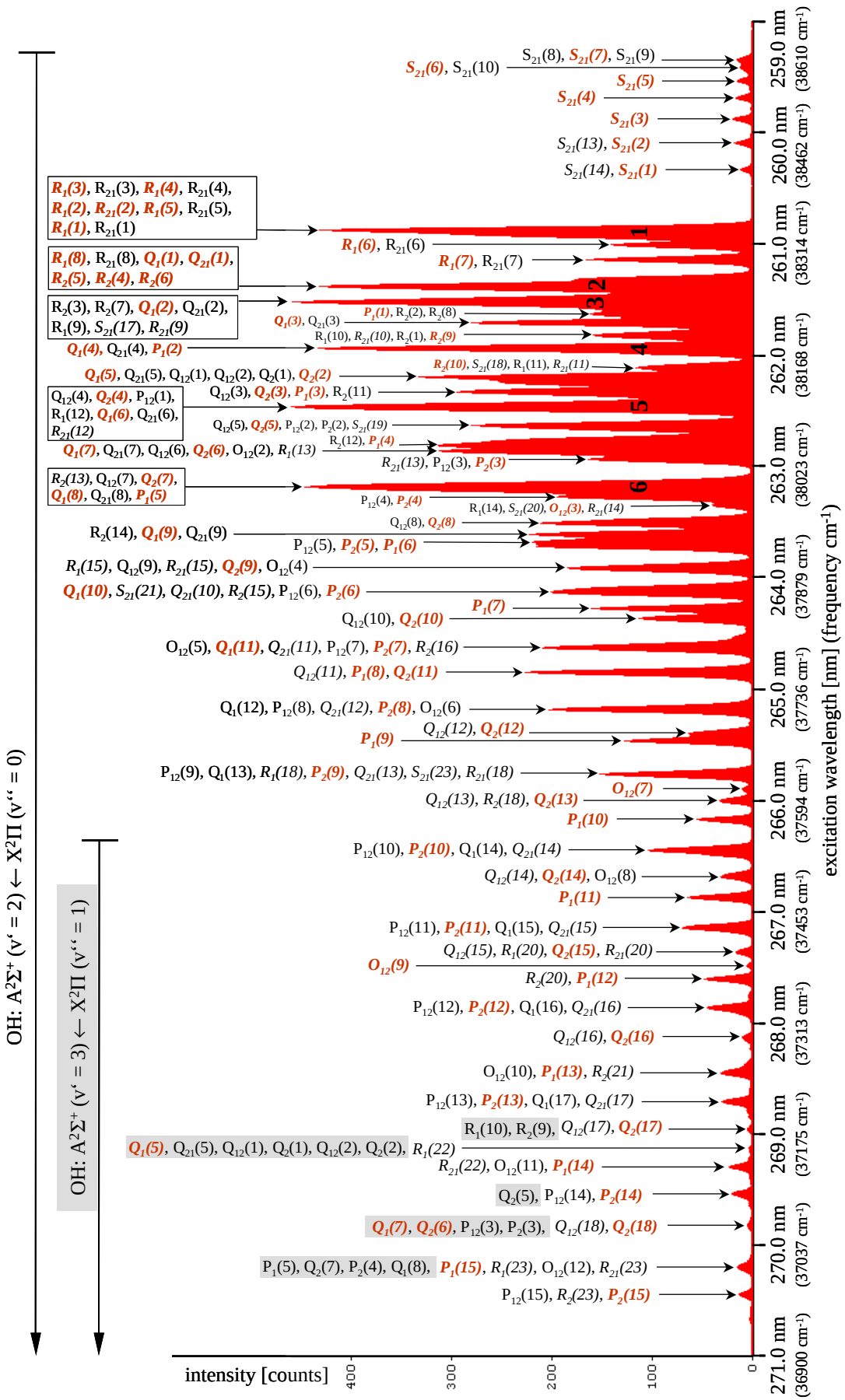

Fig. 11: Excitation spectrum of hydroxyl in a methane/air flame within the excitation wavelength range of 271.0 nm to 259.0 nm. Fluorescence signals are averaged in the emission wavelength interval from 286.5 nm to 290.7 nm. OH peaks are labeled with the rotational lines concerned.

3.4 SUMMARY

The presented work outlines possibilities of application of a tunable OPO laser system used to study methane/air and hydrogen/oxygen flames. The excitation wavelength applied ranges from 303 nm down to 240 nm. With this method it is possible to detect laser-induced (predissociative) fluorescence (LIF, LIPF) of different kinds of species formed in combustion processes. With the OPO laser system used in the experiments, hot oxygen, nitrogen monoxide and the hydroxyl radical can be excited from the electronic ground state to higher electronic states. A selective excitation of these three species within the investigated excitation wavelength range is possible.

A comparison of OH fluorescence signal intensities shows that excitation within the $A^2\Sigma^+ \leftarrow X^2\Pi$ (1,0) band (LIF) yields ≈100 times stronger signal intensities than excitation within the (3,0) band (excitation range of the KrF excimer laser, LIPF). The excitation within the (2,0) band (LIF) yields ≈20 times more intense fluorescence signal intensities in comparison to the (3,0) band (LIPF). Because of the high level of OH fluorescence signal intensities in the (1,0) and (2,0) band it is possible to get spatial and time-resolved measurements of the OH distribution in different flames. However with the OPO laser system as described in the paper, only qualitative measurements of hydroxyl can be obtained within the (1,0) and (2,0) band, because of quenching. Fig. 12 shows an OH LIF single shot measurement in a methane/air flame of a Bunsen burner at an excitation frequency of 38322 cm^{-1}.

Further investigations will get spatial-resolved and time-resolved images of the OH and NO distribution in industrial burners.

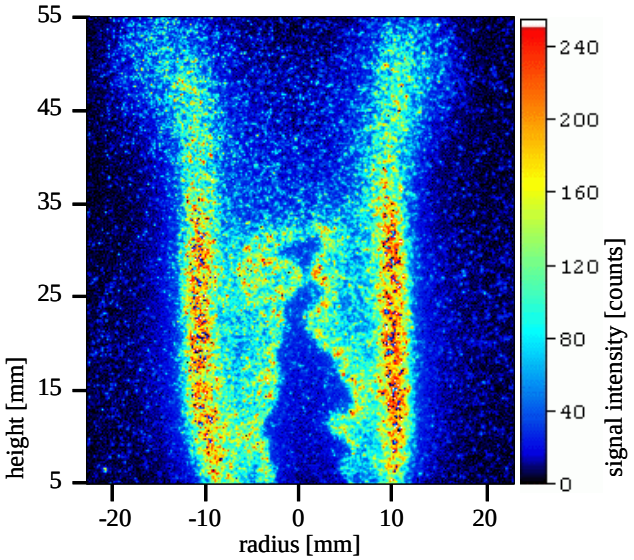

Fig. 12: OH LIF single shot measurement in a methane/air flame of a Bunsen burner. Excitation frequency at 38322 cm^{-1}.

REFERENCES

1. E. W. Rothe, and P. Andresen: "Application of tunable excimer lasers to combustion diagnostics: a review", Applied Optics Vol. 36, 3971-4033 (1996).
2. K. Kohse-Höinghaus: "Laser techniques for the quantitative detection of reactive intermediates in combustion systems", Prog. Energy Combust. Sci. 20, 203-279 (1994).
3. A. C. Eckbreth: "Laser Diagnostics for Combustion Temperature and Species", Gordon and Breach Science Publishers SA (1996).
4. A. Brockhinke, W. Kreutner, U. Rahmann, K. Kohse-Höinghaus, T. B. Settersten, and M. A. Linne: "Time-, wavelength-, and polarization-resolved measurements of OH ($A^2\Sigma^+$) picosecond laser-induced fluorescence in atmospheric-pressure flames", Appl. Phys. B 69,477-485 (1999).
5. A. Dreizler, R. Tadday, P. Monkhouse, and J. Wolfrum: "Time and spatially resolved LIF of OH $A^2\Sigma^+$ (v' = 1) in atmospheric-pressure flames using picosecond excitation", Appl. Phys. B 57,85-87 (1993).
6. H. Kobayashi, Y. Oyachi, and K. Maruta: "LIF measurements of turbulent premixed flames in a high pressure environment", Proceedings of the 5th ASME/JSME Joint Thermal Eng. Conf., AJTE99-6480 (1999).
7. M. Versluis, K. L. Queeney, J. L. Springfield, T. Dreier, and A. Dreizler: "Laser-induced fluorescence detection of OH in a flame near 268 nm", J. Mol. Spectrosc. 166, 486-488 (1994).
8. F. C. Bormann, T. Nielsen, M. Burrows, and P. Andresen: "Picosecond planar laser-induced fluorescence measurements of OH $A^2\Sigma^+$ (v' = 2) lifetime and energy transfer in atmospheric pressure flames", Applied Optics Vol. 36, 6129-6140 (1997).
9. P. Andresen, A. Bath, W. Gröger, H. W. Lülf, G. Meijer, and J. J. ter Meulen: "Laser-induced fluorescence with tunable excimer lasers as a possible method for instantaneous temperature field measurements at high pressures: checks with an atmospheric flame", Applied Optics Vol. 27, 365-378 (1988)
10. A. Koch, A. Chryssostomou, P. Andresen, and W. Bornscheuer: "Multi-species detection in spray flames with tuneable excimer lasers", Appl. Phys. B 56, 165-176 (1993).

11. A. Arnold, H. Becker, R. Hemberger, W. Hentschel, K. Kollner, W. Meienburg, P. Monkhouse, H. Neckel, M. Schafer, K. P. Schindler, V. Sick, R. Suntz, and J. Wolfrum: "Laser in situ monitoring of combustion processes", Applied Optics Vol. 29, 4860-4872 (1990).
12. E. W. Rothe, H. An, L. M. Hitchcock, Y. Gu, and G. P. Reck: "Rayleigh and predissociative fluorescence imaging of densities from an internal combustion engine using a tunable KrF laser", Laser Applications in Combustion and Combustion Diagnostics II, R. J. Locke, ed., Proc. SPIE 2122, 79-82 (1994).
13. M. Frodermann: "UV-laserspektroskopische Untersuchungen mit einem abstimmbaren Krypton-Fluorid Excimerlaser an laminaren, vorgemsichten Kohlenwasserstoff-Flammen", Ph.D. dissertation (Bielefeld University, Bielefeld, Germany), (1996).
14. C. Schulz, B. Yip, V. Sick, and J. Wolfrum: "A laser induced fluorescence scheme for imaging nitrogen oxide in engines", Chem. Phys. Lett. 242, 259-264 (1995).
15. M. Knapp, G. Grünefeld, V. Beushausen, W. Henshel, P. Andresen, A. Luczak, and S. Eisenberg: "Laserspektroskopische Diagnostik im Brennraum eines Ottomotors und an der Flamme eines Ölheizungsbrenners", VDI Ver. (Ver. Dtsch. Ing.) 1193, 325-332 (1995).
16. M. Versluis, M. Boogaarts, R. Klein-Douwel, B. Thus, W. deJongh, A. Braam, J. J. ter Meulen, W. L. Meerts, and G. Meijer: "Laser-induced fluorescence imaging in a 100 kW natural gas flame", Appl. Phys. B 55, 164-170, (1992).
17. G. Herzberg: "Molecular Spectra and Molecular Structure: 1. Spectra of Diatomic Molecules", D. Van Nostrand Company, Inc., (1967).
18. G. Herzberg: "The Spectra and Structures of Simple Free Radicals", Cornell University Press, (1971).
19. J. Luque and D. R. Crosley: "Lifbase (version 1.6)", computer program by SRI International, SRI report No. MP 99-009, (1999).